Catalytic Behavior of Nickel Particles Embedded in Three-dimensional Mesoporous SBA15

Jin-Kwon Lee, Byoung-Il An, Daniel Kim,[†] Seok-Hong Min,[‡] Jin-Seung Jung,[†] and Sung-Han Lee[*]

Department of Chemistry, Yonsei University, Wonju 220-710, Korea. [*]E-mail: shl2238@yonsei.ac.kr
[†]Department of Chemistry, Kangnung National University, Gangnung 210-702, Korea
[‡]Department of Metal and Materials Engineering, Kangnung National University, Gangnung 210-702, Korea
Received October 10, 2006

The CO_2 reforming of CH_4 has received increasing attention from both an environmental and an industrial perspective because the reaction can convert greenhouse gases into synthesis gas with a low H_2/CO ratio.[1-3] It has been known that nickel catalyst is highly active for the CO_2 reforming of CH_4, but it is easily deactivated due to coke formation and metal sintering during the reaction. To develop nickel catalyst resistant to the formation of coke, various materials such as metal oxides, mixed metal oxides, and zeolite have been examined as supports until now. Metal oxide supports are mostly used as fine powder to give large surface area. However, fine powder may be a disadvantage of its application as support because fine particles trend to agglomerate into large particles at high temperatures. In recent, several investigators have shown that mesoporous MCM41 or SBA15 compounds can be applied as catalyst support with high loading and dispersion without destroying the support pore hexagonal structure.[4-10] SBA15 compounds are more favorable to the application as catalyst support because they have mesopores with sizes of 46-300 Å and high surface area of ~800 m^2/g.[10] Moreover, the recent discovery of ordered large-pore mesoporous SBA15 compound with three dimensional mesoporous networks has extended the applications of mesoporous SBA compound in catalysis and separation because it has the advantage in the diffusion and transport of large molecules compared to one-dimensional mesopore structures.[11-19]

This paper reports the application of mesoporous SBA15 in high temperature catalysis. The SBA15 compound with three-dimensional mesoporous networks was prepared and nickel particles were embedded within the SBA15(3D). The Ni/SBA15(3D) was examined as catalyst for the CO_2 reforming of CH_4 and its catalytic results were compared with those of Ni/SiO_2 and $Ni/\gamma\text{-}Al_2O_3$ catalysts.

Experimental

The 3D-modified mesoporous SBA15 compound with interconnected channels was synthesized according to the method described by Fan *et al.*.[11] The typical procedure involves mixing the triblock copolymer Pluronic P123 ($EO_{20}PO_{70}EO_{20}$, average molecular weight 5800), water, HCl and tetraethyl orthosilicate (TEOS). The molar ratio of TEOS : $EO_{20}PO_{70}EO_{20}$: HCl : H_2O is 1 : 0.013 : 5.0 : 202. After the mixture was stirred for 2 h at 40 °C, the solid product was recovered by filtration and then, dispersed in a solution of P123 and HCl. TMB(1,3,5-trimethylbenzene) was added to this mixture and stirred for 24 h at 130 °C. Solid product was recovered by filtration and dried at room temperature in air. The external surface of SBA15 was then functionalized by immersion of SBA15 in a phenyltrimethoxysilane ethanol solution (ethanol : phenyltrimethoxysilane = 1 : 1) for 6 h at 55 °C. To remove the surfactant molecules, the solid phase was extracted with excess 2 M HCl/ethanol solution for 2 h. Nickel particles were embedded in the SBA15 by a method similar to that described in the previous paper.[20] Both the SBA15 powder and $Ni(acac)_2$ were weighed to yield 10 wt.% Ni/SBA15(3D). The SBA15 powder was slowly stirred in $Ni(acac)_2$ aqueous solution, filtered, and washed with distilled water. To maximize the extent of exchange, the ion exchange step was repeated three times. All the procedures were performed in a glove box under an argon atmosphere. Ni/SiO_2 and $Ni/\gamma\text{-}Al_2O_3$ catalysts were prepared from $Ni(NO_3)_2 \cdot 6H_2O$ (Aldrich, 5 N), SiO_2 (99.8%, Aldrich), and $\gamma\text{-}Al_2O_3$ (99.7%, Aldrich) by conventional impregnation method. Details about the preparation and characteristics of these catalysts have been given elsewhere.[2,3] To identify Ni phase in the mesopores of the SBA15(3D), X-ray powder diffraction analysis was performed for the Ni/SBA15(3D) catalyst with a Bruker D8 Advance System using Cu Kα (λ = 1.5418 Å) and a graphite monochrometer. The BET surface areas measured for the 10 wt.% Ni/SiO_2, 10 wt.% $Ni/\gamma\text{-}Al_2O_3$, and 10 wt.% Ni/SBA catalysts by nitrogen adsorption at liquid nitrogen temperature were 140, 220, and 380 m^2/g, respectively.

The catalytic reaction was carried out in a single-pass flow reactor which was made of quartz tubing with 0.8 cm inner diameter and 20 cm length. The powdered catalyst (50 mg) was well dispersed on fused-silica bed placed in the middle of the reactor. The reactor was kept in a vertical tubular furnace and a K-type thermocouple was contacted with the outside wall of the reactor next to the catalyst bed. The typical reaction mixture at ambient condition was $CH_4/CO_2/$He(4/4/2 cm^3/min). The purity of gases was greater than 99.99% and the gases were dehydrated and purified with suitable filters. The flows of the gases were controlled by

needle valves and electronic mass flow controllers. Before each activity measurement, the catalyst was calcined *in situ* at 700 °C for 1 h under oxygen flow and cooled to room temperature under He flow. The calcined catalyst was reduced again with $H_2(20\%)$/He mixture at 700 °C for 3 h and cooled to room temperature in a flow of He. The reactor temperature was ramped to the desired value using a programmable temperature controller and finally the reaction mixture was fed over the catalyst. Gaseous reactants and products were analyzed using on-line gas chromatography equipped with a thermal conductivity detector (TCD). A cold trap was placed at the reactor exit to remove water vapor from the gaseous mixture. Gas compositions were calculated using an external standard gas mixture. To get an information about the chemical species adsorbed on the catalyst surface, FT-IR spectroscopy analysis was performed by using an IR cell which was connected to the gas handling system. The IR cell was made of quartz tubing with 10 cm length and 3.0 cm diameter, heating coil was wound around the middle of the IR cell to control the temperature, and Zn-Se windows were attached to both ends of the IR cell. The reduced catalyst was pelleted with KBr (90%) as a binder and the catalyst pellet was mounted in a quartz holder within the quartz IR cell. The catalyst pellet-loaded IR cell was heated to 600 °C in a flow of He, then the CH_4/CO_2/He reaction mixture was admitted into the IR cell, and reacted at 600 °C for 1 h. After the catalytic reaction, the IR cell was cooled to 25 °C and the IR spectrum was obtained by using FT-IR spectrometer (JASCO 300E) with a resolution of 4.0 cm^{-1}. The details of measurements are described in the previous paper.[21]

Results and Discussion

The XRD pattern of the Ni/SBA15(3D) sample reduced with hydrogen at 500 °C did not show the existence of nickel particles. The FCC characteristic peaks corresponding to elemental nickel appeared upon annealing the reduced sample at 700 °C, implying the amorphous to crystalline transformation of the inserted nickel. Figure 1 exhibits the XRD pattern of the Ni/SBA15(3D) sample reduced at 700 °C with hydrogen, showing the existence of nickel phase. To investigate the catalytic activity of Ni/SBA15(3D) catalyst for the CO_2 reforming of CH_4, the reaction mixture CH_4/
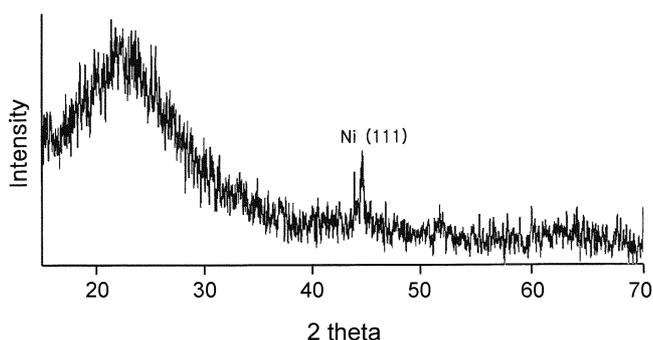
Figure 1. XRD pattern of Ni/SBA15(3D) catalyst.
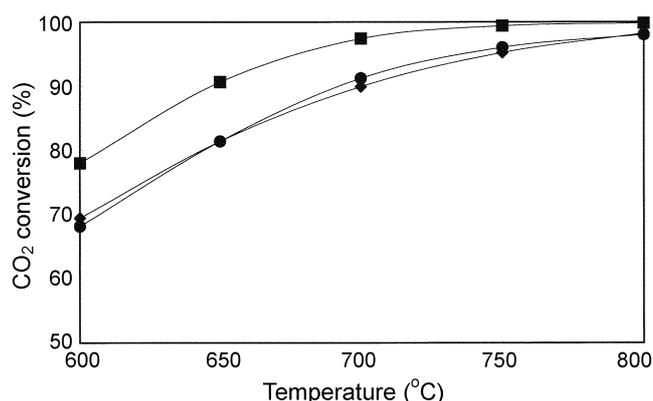
Figure 2. Variations of CO_2 conversion with temperature for 10 wt.% Ni/SiO_2 (◆), 10 wt.% $Ni/\gamma\text{-}Al_2O_3$ (■), and 10 wt.% Ni/SBA15(3D) (●) catalysts.

Figure 3. Variations of CH_4 conversion with temperature for 10 wt.% Ni/SiO_2 (◆), 10 wt.% $Ni/\gamma\text{-}Al_2O_3$ (■), and 10 wt.% Ni/SBA15(3D) (●) catalysts.

CO_2/He($4/4/2$ cm^3/min) was admitted into the reactor. In the temperature range of 600-800 °C, the Ni/SBA15(3D) catalyst showed activity for the reaction and major products were CO, H_2, and H_2O. Figures 2 and 3 compare the catalytic performances of the Ni/SiO_2, the $Ni/\gamma\text{-}Al_2O_3$, and the Ni/SBA15(3D) for the CO_2 reforming of CH_4 in the temperature range of 600-800 °C. In Figure 2, CO_2 conversions for the catalysts increase with temperature and the $Ni/\gamma\text{-}Al_2O_3$ catalyst shows the highest CO_2 conversion among the catalysts. In Figure 3, the CH_4 conversion of Ni/SBA15(3D) catalyst is lower than the other catalysts. The Ni/SBA15(3D) catalyst revealed the CO_2 conversion of 68-98% with the CH_4 conversion of 58-94% in the temperature range of 600-800 °C. The $Ni/\gamma\text{-}Al_2O_3$ catalyst showed the highest activity among the catalysts as shown in Figures 2 and 3. Figure 4 shows variations of H_2/CO ratio with temperature for the catalysts. The H_2/CO ratio increased with increasing temperature and the values were less than 1. The Ni/SBA15(3D) catalyst revealed the H_2/CO ratio of 0.55-0.98 in the temperature range of 600-800 °C. To compare the life time between the Ni/SiO_2 and the Ni/SBA15(3D) catalyst for the CO_2 reforming of CH_4, their catalytic activities were measured as a function of time-on-stream over a 30 hour period. Figure 5 shows both conver-
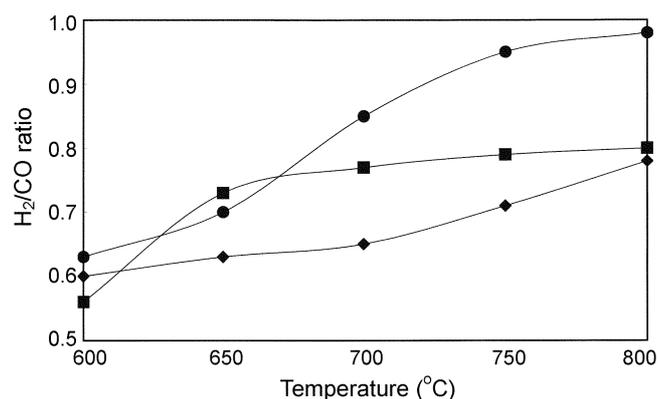
Figure 4. Variation of H_2/CO ratio with temperature for for 10 wt.% Ni/SiO_2 (◆), 10 wt.% Ni/γ-Al_2O_3 (■), and 10 wt.% $Ni/SBA15(3D)$ (●) catalysts.
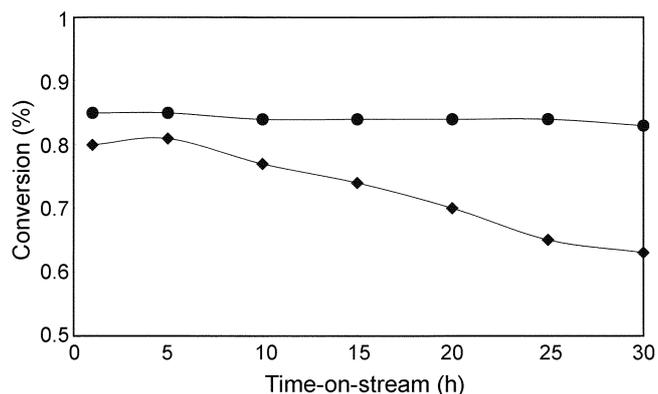
Figure 6. Variations of H_2/CO ratio with time-on-stream at 700 °C for 10 wt.% Ni/SiO_2 (◆) and 10 wt.% $Ni/SBA15(3D)$ (●) catalysts.
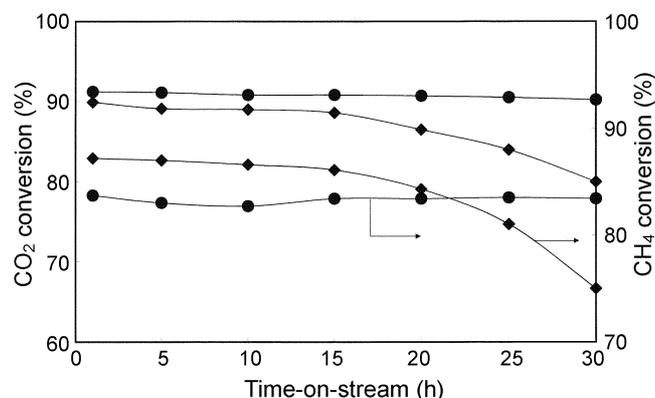
Figure 5. Variations of CO_2-conversion and CH_4-conversion with time-on-stream at 700 °C for 10 wt.% Ni/SiO_2 (◆) and 10 wt.% $Ni/SBA15(3D)$ (●) catalysts.

sions of CO_2 and CH_4 as a function of time-on-stream at 700 °C for the Ni/SiO_2 and the $Ni/SBA15(3D)$ catalyst. The Ni/SiO_2 catalyst showed that both conversions of CO_2 and CH_4 were gradually decreased along with time-on-stream, while the $Ni/SBA15(3D)$ catalyst showed nearly constant values over the extended periods, indicating that the $Ni/SBA(3D)$ catalyst is more stable than the Ni/SiO_2 catalyst for the CO_2 reforming of CH_4. The $Ni/SBA15(3D)$ catalyst also showed nearly constant H_2/CO ratio over the extended periods as shown in Figure 6. From the results, it is believed that the SBA15(3D) support enhances the stability of Ni catalyst in the CO_2 reforming of CH_4.

It has been reported that methane is stepwise decomposed into CH_x fragments on Ni surface and the CH_x intermediates with lower values of x are more likely to form carbon coke. which is responsible for the deactivation of catalyst for the catalytic CO_2-CH_4 reaction.[1-3] In this work, we found that the $Ni/SBA15(3D)$ catalyst was still active when it was again used for the CO_2-CH_4 reaction, implying the $Ni/SBA15(3D)$ catalyst to be rather resistant to coke formation. To compare the amount of carbon deposited on the catalysts during the reaction, the weight of each catalyst was measured before and after the catalytic reaction at 800 °C for 5 h.
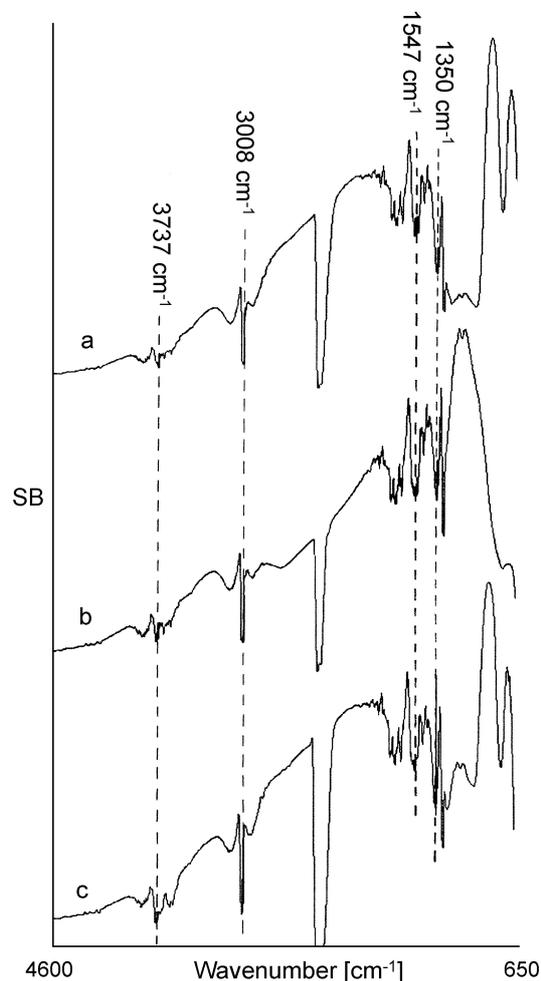
Figure 7. FT-IR spectra of the catalysts after the catalytic reaction. (a) 10 wt.% Ni/γ-Al_2O_3; (b) 10 wt.% Ni/SiO_2; (c) 10 wt.% $Ni/SBA15(3D)$.

The C/Ni mole ratios estimated for the Ni/SiO_2, the Ni/γ-Al_2O_3, and the $Ni/SBA15(3D)$ catalyst were 4.51, 2.34, and 0.29, respectively, indicating that the $Ni/SBA15(3D)$ catalyst is the most resistant to coke formation among the catalysts tested in this work. The CH_4 conversion of $Ni/$

SBA15(3D) catalyst was lower than the other catalysts as in Figure 3. The lower C/Ni mole ratio and CH_4 conversion for the Ni/SBA15(3D) catalyst enable us to consider that carbon coke is mainly produced from methane rather than CO disproportionation in the catalytic reaction and coke formation is suppressed in the pores of SBA15(3D).

Figure 7 exhibits the FT-IR spectra of catalysts after exposure to the $CH_4/CO_2/He$ mixture at 600 °C for 1 h, in which the catalysts show the same patterns on the FT-IR spectra. The IR band at 3737 cm^{-1} is attributed to the vibration of O-H in H_2O which is produced by the reaction of CO_2 and CH_4. The IR bands at 3008 and 1350 cm^{-1} are due to methyl group which is formed by the dissociative chemisorption of CH_4 and the IR band at 1547 cm^{-1} is attributed to m-CO_3^{2-} species.[22-24] It is believed from the FT-IR results that the catalytic reaction over the Ni/SBA15(3D) occurs in the same manner as the Ni/SiO_2 or Ni/γ-Al_2O_3 catalyst.

Consequently, the Ni catalyst embedded in the three-dimensional mesoporous SBA15 compound showed higher activity, lower coke formation, and higher stability than Ni catalysts supported on SiO_2 or γ-Al_2O_3 for the CO_2 reforming of CH_4 in the temperature range of 600-800 °C. The characterization of Ni particles loaded in the mesopores of SBA15(3D), the reason why coke formation is suppressed in the mesopores, and the reaction mechanism require further research to be understood and these studies are also under way.

References

 1. Bradford, M. C. J.; Vannice, M. A. *Catal. Rev.-Sci. Eng.* **1999**, *41*, 1.

 2. Yan, Q. G.; Weng, W. Z.; Wan, H. L.; Toghiani, H.; Toghiani, R. K.; Pittman Jr., C. U. *Appl. Catal. A* **2002**, *6188*, 1.

 3. Souza Mariana de, M. V. M.; Clave, L.; Dubois, V.; Carlos, A. C.; Schmal, P. M. *Appl. Catal. A* **2004**, *272*, 133.

 4. Widebmeyer, M.; Grasser, S.; Khler, K.; Anwander, R. *Micro. Meso. Mat.* **2002**, *44-45*, 327.

 5. Hsien, Y. H.; Chang, C. F.; Chen, Y. H.; Sheng, S. *Appl. Catal. B* **2001**, *31*, 241.

 6. Tuel, A.; Hubert-Pfalzgraf, L. G. *J. Catal.* **2003**, *217*, 343.

 7. Chicker, F.; Nogier, J. Ph.; Launay, F.; Bonarder, J. L. *Appl. Cata. A* **2003**, *243*, 309.

 8. Landau, M. V.; Vradman, L.; Wang, X.; Titelman, L. *Micro. Meso. Mat.* **2005**, *78*, 117.

 9. Srivastava, R.; Srinivas, D.; Ratnasamy, P. *Micro. Meso. Mat.* **2006**, *90*, 314.

10. Gmez-Reynoso, R.; Ramrez, J.; Nares, R.; Luna, R.; Murrieta, F. *Catal. Today* **2005**, *107-108*, 926.

11. Fan, J.; Yu, C.; Wang, L.; Tu, B.; Zhao, D.; Sakamoto, Y.; Terasaki, O. *J. Am. Chem. Soc.* **2001**, *123*, 12113.

12. Schmidt-Winkel, P.; Lukens, W. W.; Zhao, D. Y.; Yang, P. D.; Chmelka, B. F.; Stucky, G. D. *J. Am. Chem. Soc.* **1999**, *121*, 254.

13. Sakamoto, Y.; Kaneda, M.; Terasaki, O.; Zhao, D. Y.; Kim, J. M.; Stucky, G.; Shin, H. J.; Ryoo, R. *Nature* **2000**, *40*8, 449.

14. Lee, J.; Sohn, K.; Hyeon, T. *J. Am. Chem. Soc.* **2001**, *123*, 5146.

15. Joo, S. H.; Choi, S. J.; Oh, I.; Kwak, J.; Liu, Z.; Terasaki, O.; Ryoo, R. *Nature* **2001**, *412*, 169.

16. Zhao, D.; Feng, J.; Huo, Q.; Melosh, N.; Fredrickson, G. H.; Chmelka, B. F.; Stucky, G. D. *Science* **1998**, *279*, 548.

17. Zongtao, Z.; Sheng, D.; Xudong, F.; Douglas, A. B.; Stephen, J. P.; Yen, W. *J. Phys. Chem. B* **2001**, *105*, 6755.

18. Kim, S. W.; Son, S. U.; Lee, S. L.; Hyeon, T.; Chung, Y. K. *J. Am. Chem. Soc.* **2000**, *122*, 1550.

19. Kageyama, K.; Tamazawa, J.; Aida, T. *Science* **1999**, *285*, 2113.

20. Jung, J. S.; Lee, S. H.; Kim, Y. R.; Malkinski, L.; O'Connor, C. J. *Mater. Lett.* **2002**, *55*, 182.

21. Lee, M. J.; Jun, J. H.; Jung, J. S.; Kim, Y. R.; Lee, S. H. *Bull. Kor. Chem. Soc.* **2005**, *26*(10), 1591.

22. Wan, H. L.; Zhou, X. P.; Weng, W. Z.; Long, R. Q.; Chao, Z. S.; Zheng, W. D.; Luo, J. Z.; Zhou, S. Q. *Catal. Today* **1999**, *51*, 161.

23. Li, C.; Li, G.; Xin, Q. *J. Phys. Chem.* **1994**, *98*, 1933.

24. Li, Z.; Xu, G.; Hoflund, G. B. *Fuel Pro. Tech.* **2003**, *84*, 1.